2016

HFO1234ze(E) Boiling Inside a Brazed Plate Heat Exchanger

Giovanni A. Longo
University of Padova, Italy, tony@gest.unipd.it

Simone Mancin
University of Padova, Italy, simone.mancin@unipd.it

Giulia Righetti
University of Padova, Italy, giuliarighetti@gmail.com

Claudio Zilio
University of Padova, Italy, claudio.zilio@unipd.it

HFO1234ze(E) Boiling Inside a Brazed Plate Heat Exchanger

Giovanni A. LONGO*, Simone MANCIN, Giulia RIGHETTI, Claudio ZILIO

University of Padova, Department of Management and Engineering
I-36100 Vicenza, Italy
Phone: +39 444 998726, Fax: +39 444 998888, E-mail: tony@gest.unipd.it

* Corresponding Author

ABSTRACT

This paper investigates the effects of heat flux, saturation temperature, and outlet conditions on HFO1234ze(E) boiling inside a Brazed Plate Heat Exchanger (BPHE). The heat transfer coefficients show great sensitivity to heat flux and outlet conditions and weak sensitivity to saturation temperature (pressure). The frictional pressure drop shows a linear dependence on the refrigerant kinetic energy per unit volume. The two-phase flow boiling heat transfer coefficients were compared with a new model for refrigerant boiling inside BPHE (Longo *et al.*, 2015): the mean absolute percentage deviation between calculated and experimental data is 7.2%. The present data points were compared with those of HFC134a and HFO1234yf previously measured inside the same BPHE under the same operating conditions: HFO1234ze(E) exhibits heat transfer coefficients very similar to HFC134a and HFO1234yf and frictional pressure drops slightly higher than HFC134a and HFO1234yf.

1. INTRODUCTION

HFC134a has been probably the most important refrigerant of the two past decades as it dominated the applications in domestic refrigeration, mobile air conditioning and large chillers and it took part as component in several refrigerant mixtures such as HFC404A, and HFC407C.
Unfortunately HFC134a exhibits a relatively large, 1300, Global Warming Potential (GWP), and it will be subjected to a gradual reduction in the use up to a complete phase out in the near future according to the different national and international regulations. For example the most recent release of the EU F-gas regulation (Regulation (EU) No 517/2014) established the complete phase out of HFC134a in domestic refrigeration and mobile air-conditioning systems since January 1st, 2015 and in centralised refrigeration systems since January 1st, 2022. Therefore it is essential to identify low GWP replacements for HFC134a.
The HydroFluoroOlefin (HFO) refrigerants HFO1234yf and HFO1234ze(E) seem to be the most promising candidates as they exhibit very low GWP values (1 or less) together with pressure and volumetric properties closely near to those of HFC134a. The unique drawback of HFO refrigerants seems to be their mild flammability (Class A2L of ANSI / ASHRAE Standard 34, 2013). The Brazed Plate Heat Exchangers (BPHEs), which involve a reduction of the refrigerant charge of one order of magnitude as compared to the traditional tubular heat exchangers, are particularly interesting for limiting the risk of flammable or mildly flammable refrigerants such as HFOs (Palm, 2007). In fact the first attempt to reduce the risk of flammable refrigerants is to decrease the refrigerant charge.
The authors of the present paper had already tested HFO1234yf both in condensation and vaporisation inside a BPHE and compared its performance to those of HFC134a (Longo, 2012; Longo and Zilio, 2013). They had also carried out experimental tests on HFO1234ze(E) condensation inside a BPHE (Longo *et al.*, 2014). This paper presents the heat transfer coefficients and pressure drops measured during HFO1234ze(E) vaporisation inside a BPHE: the effects of heat flux, saturation temperature, and outlet conditions are investigated.

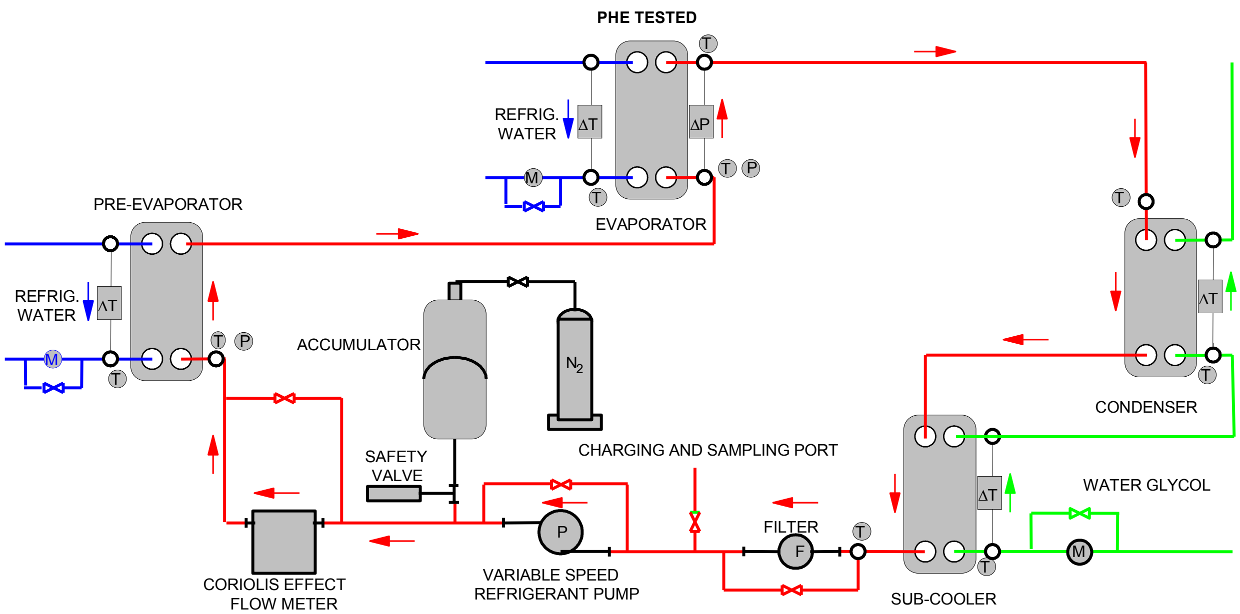

Figure 1: Schematic view of the experimental rig

2. EXPERIMENTAL SET-UP AND PROCEDURES

The experimental facility, shown in Figure 1, consists of three different circuits: one for the refrigerant and two for the secondary fluids (water and an aqueous ethylene glycol solution). The evaporator tested is a BPHE consisting of 10 plates, 72 mm in width and 278 mm in length, which present a macro-scale herringbone corrugation with an inclination angle of 65° and a corrugation amplitude of 2 mm. Figure 2 and Table 1 give the main geometrical characteristics of the BPHE tested, whereas Table 2 outlines the main features of the different measuring devices in the experimental rig. A detailed description of the experimental rig, the measurement devices and the operating procedures is reported by Longo and Gasparella (2007). The experimental results are reported in terms of boiling heat transfer coefficients and frictional pressure drop.

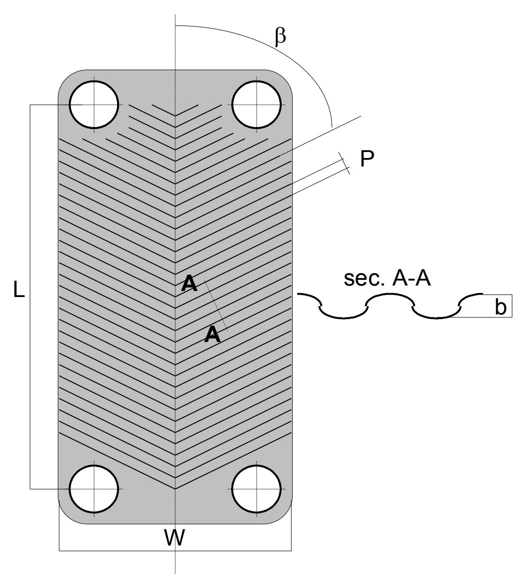

Figure 2: Schematic view of the plate

Table 1: Geometrical characteristics of the BPHE

Fluid flow plate length L(mm)	278.0
Plate width W(mm)	72.0
Area of the plate A(m^2)	0.02
Enlargement factor Φ	1.24
Corrugation type	Herringbone
Angle of the corrugation β(°)	65
Corrugation amplitude b(mm)	2.0
Corrugation pitch p(mm)	8.0
Number of plates	10
Number of effective plates N	8
Channels on refrigerant side	4
Channels on water side	5

Table 2: Specification of the different measuring devices

Device	**Type**	**Uncertainty (k= 2)**	***Range***
Thermometer	T-type thermocouple	0.1 K	-20 / 80°C
Differential thermometer	T-type thermopile	0.05 K	-20 / 80°C
Abs. pressure transducer	Strain-gage	0.075% f.s.	0 / 1.0 MPa
Diff. pressure transducer	Strain-gage	0.075% f.s.	0 / 0.3 MPa
Refrigerant flow meter	Coriolis effect	0.1% measured value	0 / 300 kg/h
Water flow meter	Magnetic	0.15% f.s.	100 / 1200 l/h

3. DATA REDUCTION

The boiling heat transfer coefficient h_r is computed from the overall heat transfer coefficient U by determining the water side heat transfer coefficient h_w.

$$h_r = (1 / U - s / \lambda_p - 1 / h_w)^{-1} \tag{1}$$

The overall heat transfer coefficient in the evaporator U is equal to the ratio between the heat flow rate Q, the nominal heat transfer area S and the logarithmic mean temperature difference ΔT_{ln}

$$U = Q / (S\ \Delta T_{ln}) \tag{2}$$

The heat flow rate is derived from a thermal balance on the waterside of the evaporator:

$$Q = m_w\ c_{pw}\ |\Delta T_w| \tag{3}$$

where m_w is the water mass flow rate, c_{pw} the water specific heat capacity and $|\Delta T_w|$ the absolute value of the temperature variation on the water side of the evaporator. The nominal heat transfer area of the evaporator

$$S = N\ A \tag{4}$$

is equal to the nominal projected area $A = L \times W$ of the single plate multiplied by the number N of the effective elements in heat transfer, as suggested by Shah and Focke (1988).
When the evaporator works only in two-phase heat transfer the logarithmic mean temperature difference is equal to:

$$\Delta T_{ln}=(T_{wi}-T_{wo}) / ln[(T_{wi}-T_{sat})/(T_{wo}-T_{sat})] \tag{5}$$

where T_{sat} is the average saturation temperature of the refrigerant derived from the average pressure measured on refrigerant side and T_{wi} and T_{wo} the water temperatures at the inlet and the outlet of the evaporator. When the evaporator works both in vaporisation and super-heating, Dutto *et al.* (1991) and Fernando *et al.* (2004) suggested the following expression for the logarithmic mean temperature difference:

$$\Delta T_{ln}=Q / [(Q_{boil} / \Delta T_{ln.boil})+(Q_{sup} / \Delta T_{ln.sup})] \tag{6}$$

where

$$Q_{boil}=m_w c_{pw}(T_{wm}-T_{wo}) \tag{7}$$

$$Q_{sup}=m_w c_{pw}(T_{wi}-T_{wm}) \tag{8}$$

are the heat flow rate exchanged in the boiling and super-heating zones respectively,

$$\Delta T_{ln.boil}=(T_{wm}-T_{wo}) / ln[(T_{wm}-T_{sat})/(T_{wo}-T_{sat})] \tag{9}$$

$$\Delta T_{ln.sup}=[(T_{wi}-T_{rout})-(T_{wm}-T_{sat})] / ln[(T_{wi}-T_{rout})/(T_{wm}-T_{sat})] \tag{10}$$

are the logarithmic mean temperature difference in the boiling (eq. 9) and super-heating (eq. 10) zones respectively, whereas T_{wm} is the water temperature between the super-heating and the boiling zone and T_{rout} is the refrigerant temperature at the outlet of the evaporator. The water temperature between the super-heating and the boiling zone is calculated from:

$$T_{wm} = T_{wi} - m_r\ c_{pVr}\ (T_{rout} - T_{sat}) / (m_w\ c_{pw}) \tag{11}$$

where m_r is the refrigerant mass flow rate and c_{pVr} is the specific heat capacity of the refrigerant vapour. This approach computes the overall heat transfer coefficient of the evaporator U as the average value between the overall heat transfer coefficient of the boiling zone U_{boil} and that of the super-heating zone U_{sup} weighted on the base of the respective heat transfer area. In this way it is possible to directly compare the heat transfer performance of an evaporator working only in two-phase heat transfer with that of an evaporator working also in vapour super-heating.
The water side heat transfer coefficient h_w is computed by the following non-dimensional equation:

$$h_w = 0.277\ (\lambda_w / d_h)\ \mathrm{Re}_w^{0.766}\ \mathrm{Pr}_w^{0.333} \tag{12}$$

$$5 < \mathrm{Pr}_w < 10 \qquad\qquad 200 < \mathrm{Re}_w < 1200$$

implemented by means of a modified Wilson plot technique as suggested by Muley and Manglik (1999). The detailed description of this procedure is reported by Longo and Gasparella (2007).
The refrigerant vapour quality at the evaporator inlet and outlet X_{in} and X_{out} are computed starting from the refrigerant temperature $T_{pb.in}$ and pressure $p_{pb.in}$ at the inlet of the pre-evaporator (sub-cooled liquid condition) considering the heat flow rate exchanged in the pre-evaporator and in the evaporator Q_{pb} and Q and the pressure at the inlet and outlet p_{in} and p_{out} of the evaporator as follows:

$$X_{in} = f(J_{in}, p_{in}) \tag{13}$$

$$X_{out} = f(J_{out}, p_{out}) \tag{14}$$

$$J_{in} = J_{pb.in}\,(T_{pb.in}, p_{pb.in}) + Q_{pb} / m_r \tag{15}$$

$$J_{out} = J_{in} + Q / m_r \tag{16}$$

$$Q_{pb} = m_{pb.w}\ c_{pw}\ |\Delta T_{pb.w}| \tag{17}$$

where J is the specific enthalpy of the refrigerant, m_r the refrigerant mass flow rate, $m_{pb.w}$ the water mass flow rate and $|\Delta T_{pb.w}|$ the absolute value of the temperature variation on the water side of the pre-evaporator.
During the experimental tests with super-heated vapour at the evaporator outlet, it is possible to compare the thermal balance on the waterside to the thermal balance on the refrigerant side from the pre-evaporator inlet (sub-cooled liquid) to the evaporator outlet (super-heated vapour). The difference between the two thermal balances was always less than 4%.
The frictional pressure drop on the refrigerant side Δp_f is computed by subtracting the manifolds and ports pressure drops Δp_c, the momentum pressure drops Δp_a and the gravity pressure drops Δp_g from the total pressure drop measured Δp_t:

$$\Delta p_f = \Delta p_t - \Delta p_c - \Delta p_a - \Delta p_g \tag{18}$$

The momentum and gravity pressure drops are estimated by the homogeneous model for two-phase flow as follows:

$$\Delta p_a = G^2 (v_V - v_L)\ |\Delta X| \tag{19}$$

$$\Delta p_g = g\ \rho_m\ L \tag{20}$$

where G is the refrigerant mass flux, v_L and v_V are the specific volume of liquid and vapour phase, $|\Delta X|$ is the absolute value of the vapour quality change between inlet and outlet and

$$\rho_m = [X_m / \rho_V + (1 - X_m) / \rho_L]^{-1} \tag{21}$$

is the average two-phase density between inlet and outlet calculated by the homogeneous model at the average vapour quality X_m between inlet and outlet. The manifold and port pressure drops are empirically estimated, in accordance with Shah and Focke (1988), as follows

$$\Delta p_c = 1.5\ G^2 / (2\ \rho_m) \tag{22}$$

The refrigerant properties are evaluated by the NIST Standard Reference Database REFPROP 9.1 (Lemmon *et al.*, 2013).

Table 3: Operating conditions during experimental tests

Runs	T_{sat}(°C)	p_{sat}(MPa)	X_{in}	X_{out}	ΔT_{sup}(°C)	G_r(kg m^{-2}s^{-1})	G_w(kg m^{-2}s^{-1})	q(kWm^{-2})
138	9.9–20.2	0.30–0.43	0.19–0.30	0.79–1.00	4.6–10.3	11.1–31.4	49.0–141.9	3.7–16.7

4. ANALYSIS OF THE RESULTS

The experimental data consists of 138 vaporisation runs carried out at three different vaporisation temperatures (10, 15, and 20 °C) and four different evaporator outlet conditions (saturated mixtures with vapour quality of 0.80 and 1.00, super-heated vapour with super-heating of 5 and 10 °C), Table 3 shows the main operating conditions during the experimental tests: refrigerant saturation temperature T_{sat} and pressure p_{sat}, inlet and outlet refrigerant vapour quality X_{in} and X_{out}, outlet refrigerant super-heating ΔT_{sup}, refrigerant mass flux G_r, water mass flux G_w, and heat flux q. The operating conditions investigated are typical for evaporators of vapour compression chillers and heat pumps in air conditioning application (Palm and Claesson, 2006). A detailed error analysis performed in accordance with Kline and McClintock (1953) indicates an overall uncertainty within ±12.0% for the refrigerant heat transfer coefficient measurement and within ±6.6% for the total pressure drop measurement.

Figures 3, 4, and 5 show the boiling heat transfer coefficients against heat flux at three different evaporation temperatures (10, 15 and 20 °C) and four different evaporator outlet conditions (vapour quality around 0.80 and 1.00, vapour super-heating around 5 and 10 °C). The heat transfer coefficients show great sensitivity to heat flux and outlet conditions and weak sensitivity to saturation temperature (pressure). The boiling heat transfer coefficients with 0.80 outlet vapour quality are 6-11% higher than those with 1.00 outlet vapour quality, 13-16% higher than those with 5 °C of outlet vapour super-heating, and 39-46% higher than those with 10 °C of outlet vapour super-heating. The inception of the dry-out might justify the slight decrease of the boiling heat transfer coefficient when outlet vapour quality increases from 0.80 to 1.00, whereas the increase of the outlet vapour super-heating involves a considerable degradation of the boiling heat transfer coefficients.

The experimental two-phase flow boiling heat transfer coefficients were compared against traditional equations for nucleate boiling, such as Cooper (1984) and Gorenflo (1993), and also against a recent model specifically developed for refrigerant vaporisation inside BPHEs by Longo *et al*. (2015).

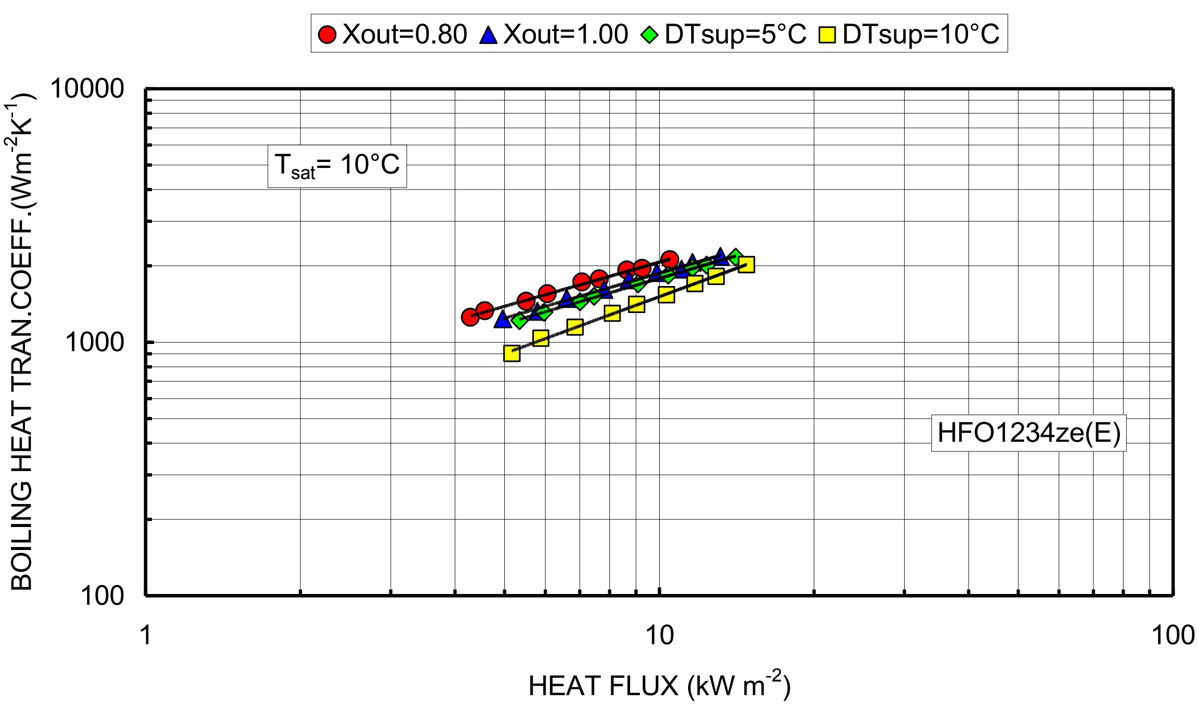

Figure 3: Boiling heat transfer coefficient on refrigerant side vs. heat flux at 10°C

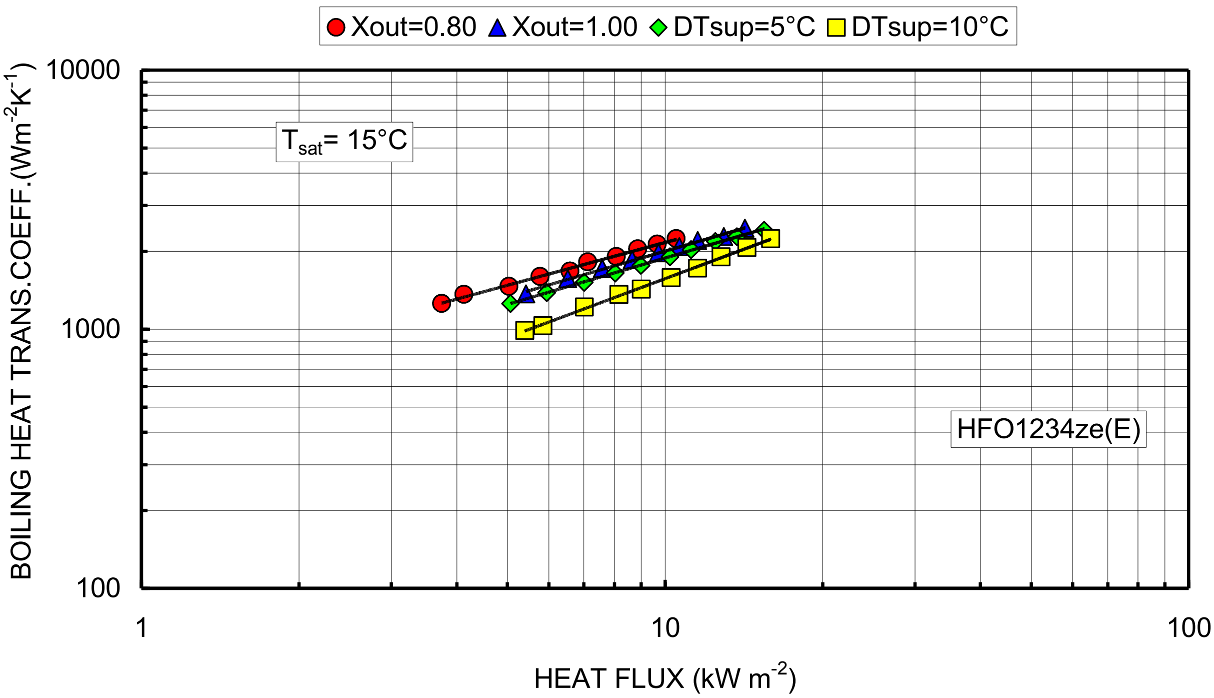

Figure 4: Boiling heat transfer coefficient on refrigerant side vs. heat flux at 15°C

The absolute mean percentage deviation between calculated and experimental data is 13.4%, 13.1%, and 7.1% for Cooper (1984) equation, Gorenflo (1993) equation, and Longo *et al*. (2015) model, respectively. Figure 6 shows the comparison between the experimental two-phase flow boiling heat transfer coefficients and the calculated values by Longo et *al*. (2015).

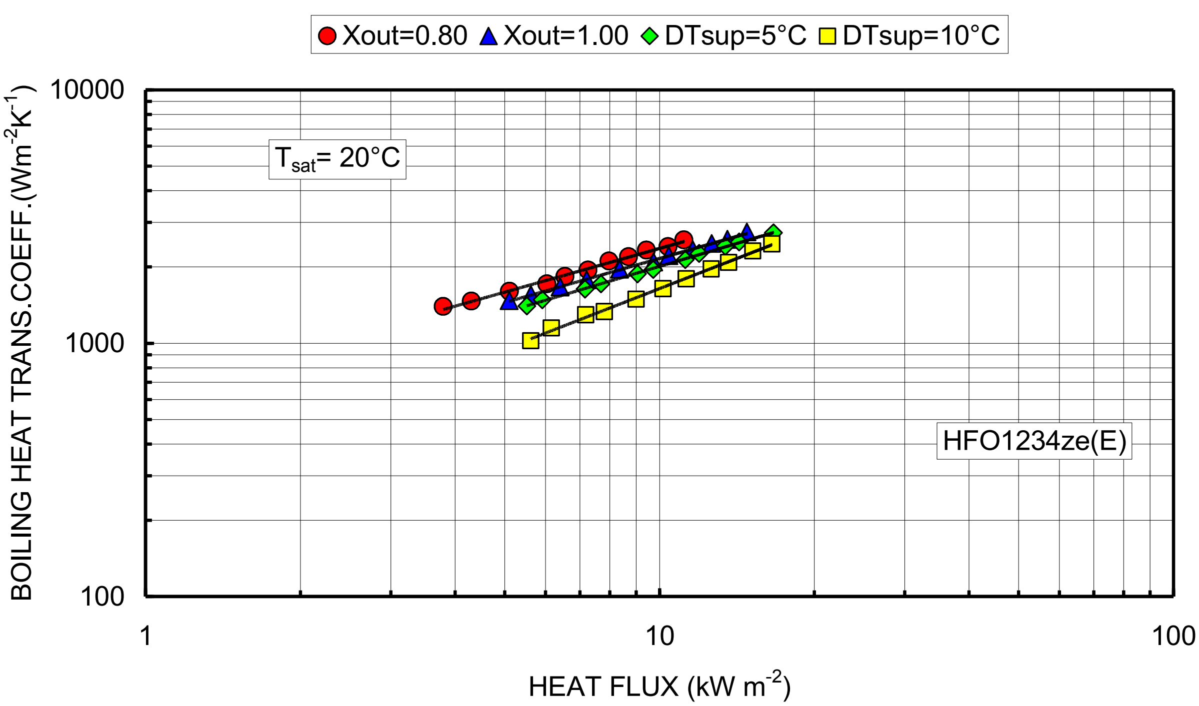

Figure 5: Boiling heat transfer coefficient on refrigerant side vs. heat flux at 20°C

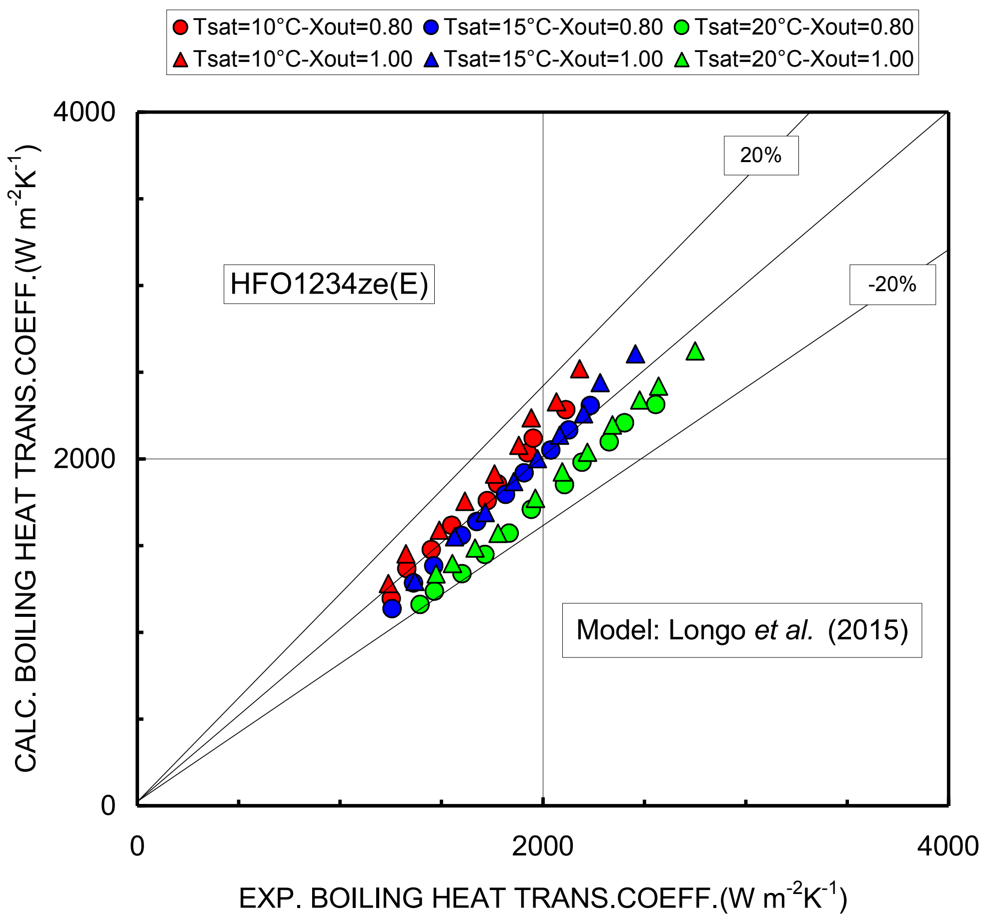

Figure 6: Comparison between experimental and calculated heat transfer coefficients by Longo *et al*. (2015) model

Figure 7 shows the two-phase flow boiling frictional pressure drop against the kinetic energy per unit volume of the refrigerant flow computed by the homogeneous model:

$$KE/V = G^2 / (2\,\rho_m) \tag{23}$$

It is possible to observe a fairly linear dependence of the frictional pressure drop on the kinetic energy per unit volume of the refrigerant flow as already found by Jassim *et al*. (2006) in adiabatic two-phase flow of HFC134a through a BPHE with herringbone and bumpy corrugation. The following best fitting linear correlation was derived from present experimental data:

$$\Delta p_f\,[\mathrm{kPa}] = 1.667\ KE/V\,[\mathrm{J\ m^{-3}}] \tag{24}$$

This linear correlation reproduces present set of experimental data points with a mean absolute percentage deviation around 7.2%.
HFO1234ze(E) and HFO1234yf are probably the most promising replacements for HFC134a, therefore it is interesting to compare their thermal and hydraulic performance to those of HFC134a. Present HFO1234ze(E) data points were compared with those of HFO1234yf and HFC134a previously measured by the present authors (Longo, 2012; Longo and Gasparella, 2007) inside the same BPHE under the same operating conditions. HFO1234ze(E) exhibits heat transfer coefficients very similar to HFC134a and HFO1234yf and frictional pressure drops slightly higher than HFC134a and HFO1234yf. This can be attributed mainly to the lower absolute pressure and the higher vapour specific volume of HFO1234ze(E) with respect to both HFC134a and HFO1234yf.

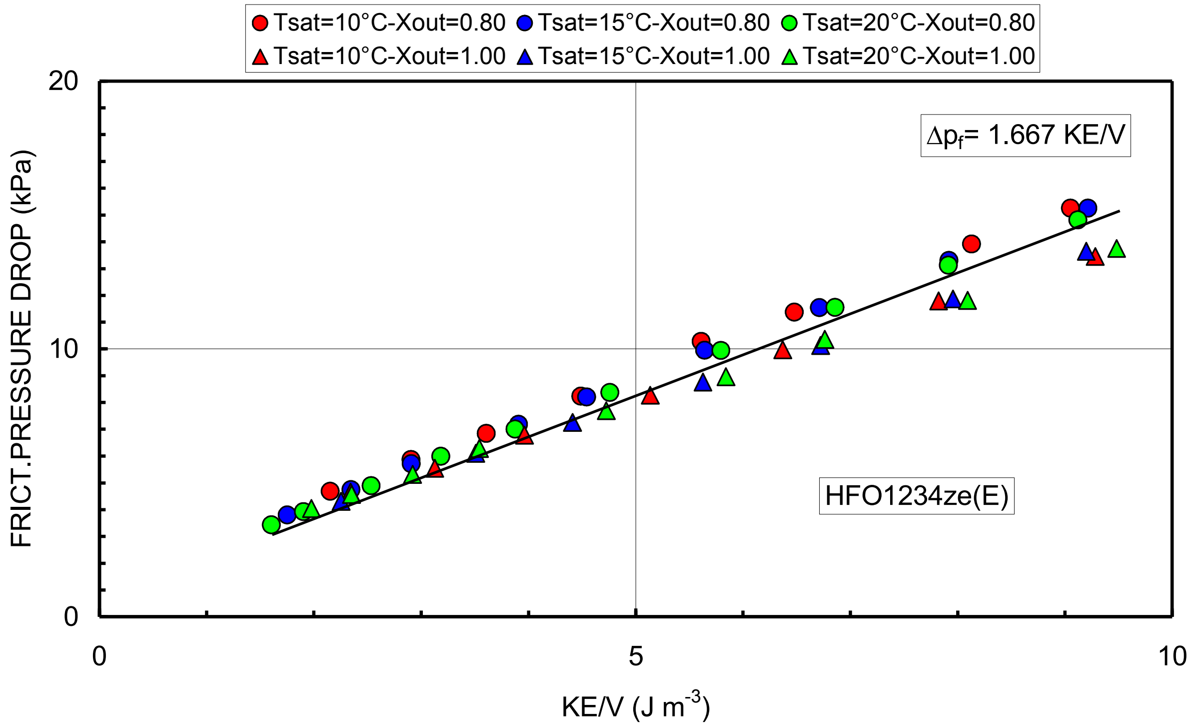

Figure 7: Frictional pressure drop vs. kinetic energy per unit volume

6. CONCLUSIONS

This paper investigates the effects of heat flux, saturation temperature, and outlet conditions on HFO1234ze(E) boiling inside a BPHE. The heat transfer coefficients show great sensitivity to heat flux and outlet conditions and weak sensitivity to saturation temperature (pressure). The two-phase flow boiling heat transfer coefficients are 39-46% higher than those with 10 °C of outlet super-heating. The frictional pressure drop shows a linear dependence on the kinetic energy per unit volume of the refrigerant flow and therefore a quadratic dependence on refrigerant mass flux. The two-phase flow boiling heat transfer coefficients are in fair agreement with a recent model for refrigerant vaporisation inside BPHEs (Longo *et al*., 2015): the absolute mean percentage deviation between calculated and experimental data is 7.1%.
HFO1234ze(E) exhibits boiling heat transfer coefficients very similar to HFC134a and HFO1234yf and frictional pressure drop slightly higher than HFC134a and HFO1234yf. Based on the discussed results, it can be concluded that HFO1234ze(E) has potential to be a substitute of HFC134a, and a suitable alternative to HFO1234yf also in applications adopting BPHE as evaporator.

NOMENCLATURE

A	nominal area of a plate	(m^2)
b	height of the corrugation	(m)
c_p	specific heat capacity	(J kg^{-1}K^{-1})
d_h	hydraulic diameter, $d_h = 2\,b$	(m)
f.s.	full scale	
g	gravity acceleration	(m s^{-2})
G	mass flux, $G = m \,/\, (n_{ch}\, W\, b)$	(kg m^{-2}s^{-1})
h	heat transfer coefficient	(W m^{-2}K^{-1})
J	specific enthalpy	(J kg^{-1})

k	coverage factor	
KE/V	kinetic energy per unit volume	(J m^{-3})
L	flow length of the plate	(m)
m	mass flow rate	(kg s^{-1})
n_{ch}	number of channels	
$\boldsymbol{N}$	**number of effective plates**	
p	pressure	(Pa)
$\boldsymbol{P}$	**co**rrugation pitch	(**m**)
Pr	Prandtl number, Pr = $\mu c_p / \lambda$	
q	heat flux, $q = Q / S$	(Wm^{-2})
Q	heat flow rate	(W)
R_a	arithmetic mean roughness (ISO 4271/1)	(µm)
Re	Reynolds number, Re = $G d_h / \mu$	
R_p	roughness (DIN 4762/1)	(µm)
S	nominal heat transfer area, m^2	
s	plate wall thickness	(m)
T	temperature, K	
U	overall heat transfer coefficient	($Wm^{-2}K^{-1}$)
v	specific volume	(m^3kg^{-1})
W	width of the plate	(m)
X	vapour quality, $X = (J - J_L) / \Delta J_{LV}$	

Greek symbols

β	inclination angle of the corrugation	(°)
λ	thermal conductivity	(W $m^{-1}K^{-1}$)
μ	viscosity	(kg $m^{-1}s^{-1}$)
ρ	density	(kg m^{-3})
Δ	difference	
ΔJ_{LV}	latent heat of vaporisation	(J kg^{-1})
Φ	enlargement factor	

Subscript

a	momentum
c	manifolds and ports
f	frictional
g	gravity
in	inlet
L	liquid phase
LV	liquid vapour phase change
ln	logarithmic
out	outlet
p	plate
pb	pre-evaporator
r	refrigerant
sat	saturation
sup	super-heating
t	total
V	vapour phase
w	water
wi	water inlet
wm	water between the super-heating and the boiling zone
wo	water outlet

REFERENCES

ANSI / ASHRAE 34, 2013. Designation and Safety Classification of Refrigerants.

Cooper, M.G., 1984. Heat flows rates in saturated pool boiling - a wide ranging examination using reduced properties. In: Advanced in Heat Transfer. Academic Press, Orlando, Florida, pp. 157-239.

Dutto, T., Blaise, J.C., Benedic, T., 1991. Performances of brazed plate heat exchanger set in heat pump. In Proc. of 18th Int. Congr. Refrigeration, Montreal, Canada, pp. 1284-1288.

EU, 2014. Regulation (EU) No 517/2014 of the European Parliament and of the Council of 16 April 2014 on fluorinated greenhouse gases and repealing Regulation (EC) No 842/2006.

Fernando, P., Palm, B., Lundqvist, P., Granryd, E., 2004. Propane heat pump with low refrigerant charge: design and laboratory tests. Int. J. Refrigeration, 27, 761-773.

Gorenflo, D., 1993. Pool boiling. VDI Heat Atlas, Dusseldorf, Germany, Ha1-25.

Jassim, E.W., Newell, T.A., Chato, J.C., 2006. Refrigerant pressure drop in chevron and bumpy style flat plate heat exchangers. Exp. Therm. Fluid Sci., 30, 213-222.

Kline, S.J., McClintock, F.A., 1953. Describing uncertainties in single-sample experiments. Mech.Eng. 75, 3–8.

Lemmon, E.W., Huber, M.L, McLinden, M.O., 2013. NIST Standard Reference Database23: Reference fluid Thermodynamic and Transport Properties - REFPROP Version 9.1, NIST, Gaithersburgh MD.

Longo, G.A., Gasparella, A., 2007. Refrigerant R134a vaporisation heat transfer and pressure drop inside a small brazed plate heat exchanger. Int. J. Refrigeration, 30, 821–830.

Longo, G.A., 2012. Vaporisation of the low GWP refrigerant HFO1234yf inside a brazed plate heat exchanger. Int. J. Refrigeration, 35, 952–961.

Longo, G.A., Zilio, C., 2013. Condensation of the low GWP refrigerant HFO1234yf inside a brazed plate heat exchanger. Int. J. Refrigeration, 36, 612–621.

Longo, G.A., Zilio, C., Righetti, G., Brown, J.S., 2014. Condensation of the low GWP refrigerant HFO1234ze(E) inside a brazed plate heat exchanger. Int. J. Refrigeration, 38, 250–259.

Longo, G.A., Mancin, S., Righetti, G., Zilio, C., 2015. A new model for refrigerant boiling inside a Brazed Plate Heat Exchanger (BPHE). Int. J Heat Mass Transfer, 91, 144-149.

Muley, A., Manglik, R.M., 1999. Experimental study of turbulent flow heat transfer and pressure drop in a plate heat exchanger with chevron plates. J. Heat Transf. - Trans. ASME, 121, 110-121.

Palm, B., Claesson, J., 2006. Plate heat exchangers: calculation methods for single- and two-phase flow. Heat Transfer Eng., 27 (4), 88–98.

Palm, B., 2007. Refrigeration systems with minimum charge of refrigerant. Appl. Therm. Eng., 27, 1693-1701.

Shah, R.K., Focke, W.W., 1988. Plate heat exchangers and their design theory. In Heat Transfer Equipment Design, Hemisphere, Washington, 227-254.

ACKNOWLEDGEMENT

This research project was partially funded by:
CariVerona Foundation, Verona, Italy, Ricerca Scientifica e Tecnologica 2013-2014:
"*Sviluppo di innovativi processi a ridotto impatto ambientale per la conservazione e distribuzione a bassa temperatura delle derrate alimentari a salvaguardia della salute*".